AMERICAN SOCIETY FOR MICROBIOLOGY | Molecular and Cellular Biology®

RESEARCH ARTICLE

Long Noncoding RNA HOXA-AS3 Integrates NF-κB Signaling To Regulate Endothelium Inflammation

Xinxing Zhu,[b] Duchu Chen,[a,c] Yanli Liu,[e] Jinjin Yu,[d] Liang Qiao,[e] Shuibin Lin,[f] Demeng Chen,[f] Genshen Zhong,[g] Xifeng Lu,[h] Yize Wang,[a] Jieqi Wen,[a] Xinqi Zhong,[i] Yizhou Jiang[a]

[a]Institute for Advanced Study, Shenzhen University, Shenzhen, Guangdong, China
[b]Henan Joint International Research Laboratory of Stem Cell Medicine, College of Biomedical Engineering, Xinxiang Medical University, Xinxiang, Henan, China
[c]Key Laboratory of Optoelectronic Devices and Systems of Ministry of Education and Guangdong Province, College of Optoelectronic Engineering, Shenzhen University, Shenzhen, Guangdong, China
[d]School of Psychology, Xinxiang Medical University, Xinxiang, Henan, China
[e]Stem Cell and Biotherapy Engineering Research Center of Henan, College of Life Science and Technology, Xinxiang Medical University, Xinxiang, Henan, China
[f]Center for Translational Medicine, The First Affiliated Hospital, Sun Yat-sen University, Guangzhou, China
[g]Henan Collaborative Innovation Center of Molecular Diagnosis and Laboratory Medicine, School of Laboratory Medicine, Xinxiang Medical University, Xinxiang, Henan, China
[h]Department of Physiology, Shenzhen University Health Science Center, Shenzhen University, Shenzhen, Guangdong, China
[i]Neonatology Department, The Third Affiliated Hospital of Guangzhou Medical University, Guangzhou, Guangdong, China

ABSTRACT The long noncoding RNA HOXA-AS3 has recently been reported to act as a critical regulator in inflammation-linked lung adenocarcinoma. However, the roles of HOXA-AS3 in endothelium inflammation and related vascular disorders remain poorly defined. In the current study, we identified HOXA-AS3 to be a critical activator to promote NF-κB-mediated endothelium inflammation. HOXA-AS3, a chromatin-associated regulator which colocalizes with NF-κB at specific gene promoters, was found to interact with NF-κB and positively regulate its activity through control of the expression of the NF-κB inhibitor protein IκBα and the acetylation status at the K310 site of p65. More importantly, clinicopathological analysis showed that HOXA-AS3 expression has a significant positive correlation with atherosclerosis. Thus, we conclude that HOXA-AS3 may serve as a crucial biomarker for the clinical diagnosis of atherosclerosis, as well as a promising therapeutic target for the treatment of multiple inflammatory vascular diseases. In addition, this study suggests the functional importance of HOXA-AS3 in the regulation of inflammatory disorders.

KEYWORDS HOXA-AS3, NF-κB, acetylation, atherosclerosis, endothelium inflammation

Endothelium inflammation, widely regarded as a pathological process, is critically associated with diverse vascular inflammatory disorders, including atherosclerosis (1–3). Atherosclerosis, an inflammatory disease of the arterial wall, is the major cause of a number of common cardiovascular diseases, including heart attack, stroke, coronary heart disease, and so on. At the early stage of atherosclerosis, due to subendothelial retention of lipoproteins, endothelial cells (ECs) are activated and secrete numerous adhesion molecules, such as VCAM1 and ICAM1, which could facilitate monocyte recruitment to ECs. Moreover, some other proinflammatory cytokines and chemokines are produced to act as autocrine or paracrine factors to foster an inflammatory microenvironment (4, 5), consequently leading to endothelial dysfunction and subsequent atherosclerotic lesion formation.

NF-κB signaling, one of the most important inflammatory signaling pathways, is involved in the regulation of multiple biological processes, including inflammation,

Citation Zhu X, Chen D, Liu Y, Yu J, Qiao L, Lin S, Chen D, Zhong G, Lu X, Wang Y, Wen J, Zhong X, Jiang Y. 2019. Long noncoding RNA HOXA-AS3 integrates NF-κB signaling to regulate endothelium inflammation. Mol Cell Biol 39:e00139-19. https://doi.org/10.1128/MCB.00139-19.

Address correspondence to Xinxing Zhu, zhuxinxing0202@163.com, or Yizhou Jiang, jiangyz@szu.edu.cn.

Xinxing Zhu, Duchu Chen, and Yanli Liu contributed equally to this article.

Received 26 March 2019
Returned for modification 9 May 2019
Accepted 25 June 2019
Accepted manuscript posted online 8 July 2019
Published 11 September 2019

immunity, cell proliferation, differentiation, and survival (6–8). NF-κB, composed of homo- or heterodimers of RelA (p65), RelB, c-Rel, p50/p105 (NF-κB1), or p52/p100 (NF-κB2) (9, 10), plays a critical role in the regulation of endothelium inflammation. The aberrant activation of NF-κB can induce the expression of numerous inflammatory factors, such as the adhesion molecules VCAM1 and ICAM1 (11–13) as well as cytokines and chemokines, like interleukin-2 (IL-2), IL-8, and monocyte chemoattractant protein 1 (14, 15), which greatly contribute to monocyte recruitment to endothelial cells in the early stage of atherosclerosis and the subsequent progression of atherosclerotic plaque formation (16–19). NF-κB activity is found to be tightly regulated. Under resting conditions, NF-κB is chiefly sequestered in the cytoplasm through its assembly with inhibitor proteins of the IκB family (10). Upon proinflammatory stimulation, for instance, tumor necrosis factor alpha (TNF-α) treatment, NF-κB is liberated and translocated into the nucleus, due to the rapid ubiquitination and subsequent degradation of IκB by the 26S proteasome complex, and then it rapidly binds to κB enhancer elements and functions as a transcription factor to modulate gene transcription (9, 10). Moreover, NF-κB activity can be regulated by specific modifications at the p65 subunit, especially K310 site acetylation, which is responsible for the transcriptional activation of NF-κB (20).

Noncoding RNAs, a subset of noncoding small-molecule RNAs, have previously been reported to take part in a number of pathological processes and related diseases, such as cancers and some inflammatory cardiovascular disorders (21–23). In the past few years, a wide variety of noncoding RNA transcripts have been identified, with the development of an intensive unbiased analysis of the transcriptome (24–26). Of the noncoding RNAs, the regulatory roles of short noncoding RNAs, such as microRNAs, have been well studied. However, the long noncoding RNAs (lncRNAs), generally more than 200 nucleotides in length, accounting for the largest portion of the mammalian noncoding transcriptome, remain poorly understood due to their extremely low expression levels (27–31). The majority of lncRNAs are located in the nucleus (32). A number of the nuclear lncRNAs can directly or indirectly bind to gene promoter regions and decoy, guide, or scaffold other chromatin regulatory modifiers to mediate gene transcription (33). It has been documented that many lncRNAs are functionally involved in the progression of inflammatory vascular diseases. For example, the lncRNA ANRIL plays a regulatory role in atherosclerosis by modulating atherogenic pathways in vascular smooth muscle cells (VSMCs) (34, 35), and another lncRNA, E330013P06, can regulate foam cell formation by controlling the expression of inflammatory genes (Nos2, IL-6, and Ptgs2 genes) and scavenger receptor CD36 (26). Here, we identify the lncRNA HOXA-AS3 to be a novel positive regulator of endothelium inflammation. We demonstrate that inhibition of HOXA-AS3 dramatically represses endothelium inflammation. Mechanistically, HOXA-AS3 interacts with NF-κB and regulates its transcriptional activity by controlling the expression of IκBα and augmenting the K310 acetylation status of p65, inducing the expression of NF-κB-mediated inflammatory factors. More importantly, HOXA-AS3 was found, using clinicopathological sample analysis of carotid artery atherosclerosis, to be significantly correlated with inflammatory atherosclerosis. In summary, these observations emphasize the functional involvement of HOXA-AS3 in the regulation of inflammatory vascular diseases.

RESULTS

HOXA-AS3 positively regulates endothelium inflammation. As was previously reported, the lncRNA HOXA-AS3 can function as a critical regulator in inflammation-associated cancers (44, 45). Therefore, we hypothesized that HOXA-AS3 can regulate endothelium inflammation. To test this notion, we first performed a monocyte adhesion assay with or without HOXA-AS3 knockdown in human umbilical vein endothelial cells (HUVECs) to characterize the role of HOXA-AS3 in endothelium inflammation. As a consequence, we found that the attenuation of HOXA-AS3 can significantly impair proinflammatory TNF-α-induced THP-1 monocyte adhesion to HUVECs (Fig. 1a). To further confirm this result, we constructed a lentiviral vector and performed lentivirus

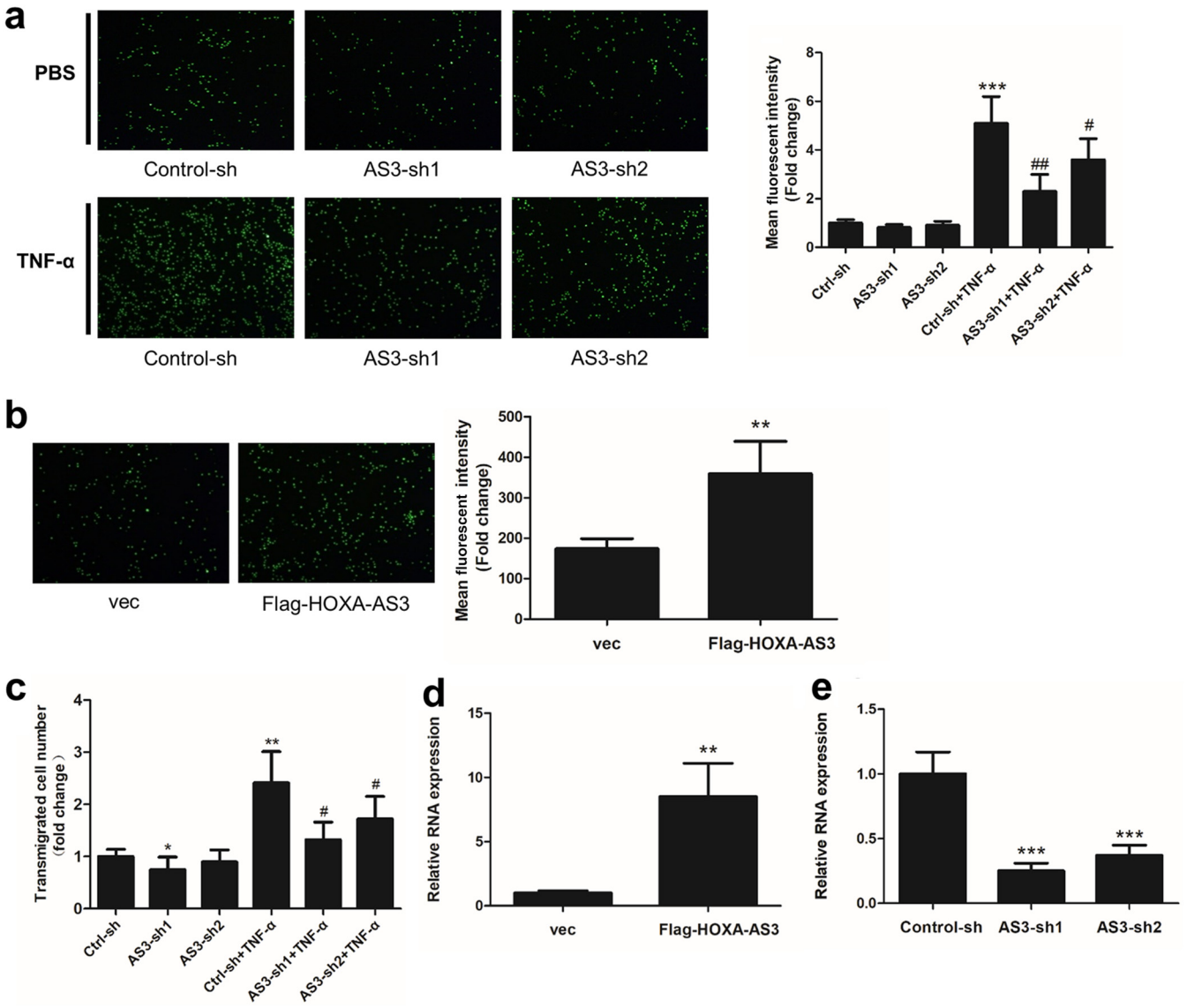

FIG 1 HOXA-AS3 promotes endothelium inflammation. (a) Fluorescence microscopy images (left) showing the effect of HOXA-AS3 inhibition on monocyte adhesion to ECs, quantified using ImageJ software (right). CMFDA (CellTracker Green)-labeled THP-1 cells were incubated with control and HOXA-AS3-depleted HUVECs activated by TNF-α (10 ng/ml, 3 h). (b) Fluorescence microscopy images (left) showing the effect of aberrant overexpression of HOXA-AS3 on monocyte adhesion to ECs, quantified using ImageJ software (right). CMFDA (CellTracker Green)-labeled THP-1 cells were incubated with control or HOXA-AS3-overexpressing HUVECs. (c) Effect of HOXA-AS3 on THP-1 cell migration through HUVECs, measured by a transendothelial migration assay. The control and HOXA-AS3-depleted HUVECs were subjected to incubation with THP-1 cells. (d and e) The overexpression and knockdown efficiency of HOXA-AS3 were determined by qRT-PCR in HUVECs. All values are for biological triplicates, and the data shown are the mean $\pm$ SD. *, $P < 0.05$ versus control shRNA or the vector (vec); **, $P < 0.01$ versus control shRNA (control-sh) or the vector; ***, $P < 0.001$ versus control shRNA or the vector; #, $P < 0.05$ versus control shRNA plus TNF-α; ##, $P < 0.01$ versus control shRNA plus TNF-α.

infection to overexpress HOXA-AS3 in HUVECs, followed by incubation with THP-1 monocytes. As expected, enforced overexpression of HOXA-AS3 dramatically induced the capacity of HUVECs to adhere to monocytes (Fig. 1b). Furthermore, a transendothelial migration assay was employed to demonstrate the positive role of HOXA-AS3 in endothelial activation. Consistently, we found that knockdown of HOXA-AS3 obviously restrained monocyte migration through HUVEC monolayers (Fig. 1c). Based on these studies, we conclude that HOXA-AS3 is able to act as a positive regulator of endothelium inflammation.

HOXA-AS3 mediates expressions of NF-κB target genes. To dissect the molecule mechanism by which HOXA-AS3 regulates endothelium inflammation, we established expression profiles in HUVECs by high-throughput RNA sequencing analysis after

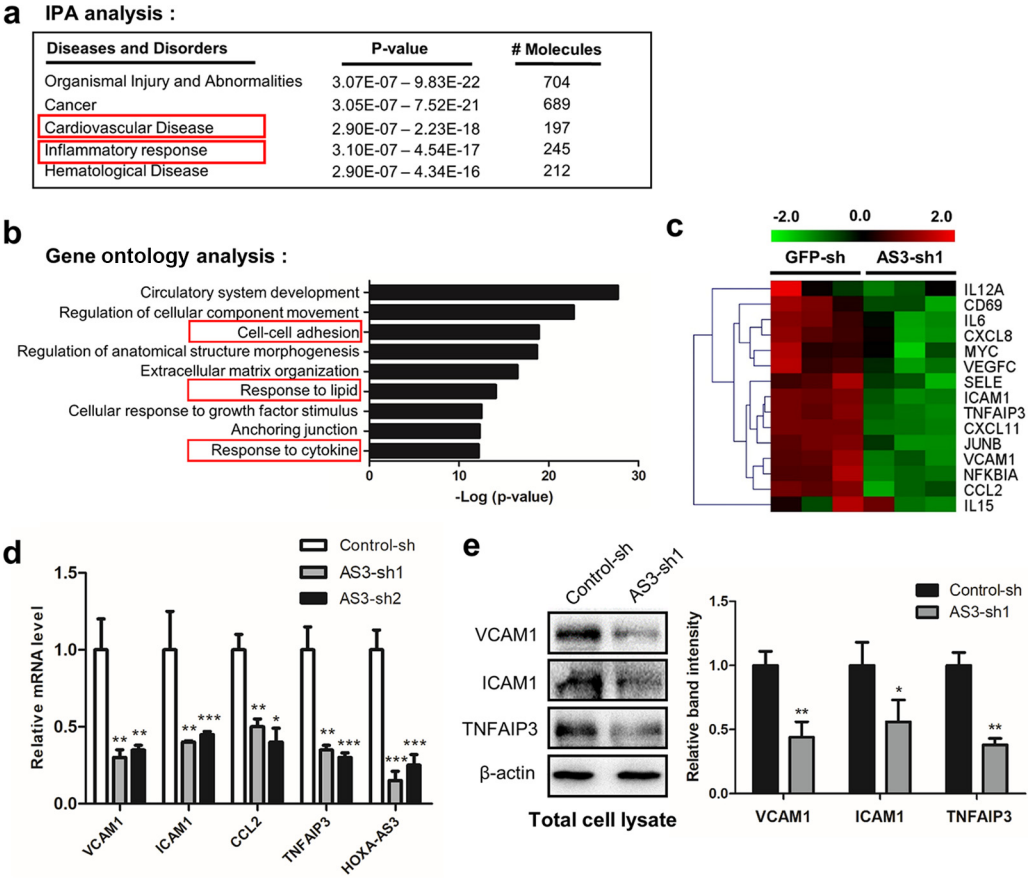

FIG 2 Knockdown of HOXA-AS3 represses expression of NF-κB target genes. (a) Ingenuity pathway analysis of the differentially expressed genes in HUVECs after HOXA-AS3 knockdown. (b) Gene ontology analysis of the differentially expressed genes in HUVECs after HOXA-AS3 knockdown. (c) Heat map of the representative NF-κB target genes that are downregulated after HOXA-AS3 knockdown. GFP-sh, shRNA targeting green fluorescent protein. (d) Effect of HOXA-AS3 on expression of VCAM1, ICAM1, CCL2, and TNFAIP3, determined by qRT-PCR in HUVECs with or without HOXA-AS3 knockdown. (e) The protein expression levels of VCAM1, ICAM1, and TNFAIP3 in HUVECs with or without HOXA-AS3 knockdown were assayed by Western blotting (left) and then quantified using ImageJ software (right). All values are from biological triplicates, and the data shown are the mean ± SD. *, $P < 0.05$ versus control shRNA; **, $P < 0.01$ versus control shRNA; ***, $P < 0.001$ versus control shRNA.

HOXA-AS3 knockdown. We found that 394 genes and 234 genes were up- and downregulated, respectively. Ingenuity pathway analysis (IPA) and Gene Ontology (GO) analysis showed that the differentially expressed genes are functionally involved in cardiovascular disease, the inflammatory response, cell-cell adhesion, and the response to lipids and cytokines (Fig. 2a and b), consistent with the above-characterized function of HOXA-AS3 in endothelial activation. Top canonical pathway analysis revealed the significant correlation between HOXA-AS3 and NF-κB signaling (data not shown). Further analysis identified that multiple up- and downregulated genes were canonical NF-κB transcriptional targets (Fig. 2c). To validate this critical discovery, we determined the expression of four representative NF-κB target genes by quantitative real-time PCR (qRT-PCR) in HUVECs and THP-1 monocytes with or without HOXA-AS3 knockdown. qRT-PCR analysis revealed that inhibition of HOXA-AS3 markedly downregulated mRNA expression of the four genes (Fig. 2d). Moreover, this finding was further confirmed by Western blot analysis at the protein level (Fig. 2e).

HOXA-AS3 interacts with NF-κB. Since HOXA-AS3 regulates the expression of NF-κB target genes, we speculated that HOXA-AS3 is involved in the regulation of NF-κB transcriptional activity. To test this notion, we first investigated the effect of HOXA-AS3 on the expression of NF-κB itself. Both qRT-PCR and Western blot analysis

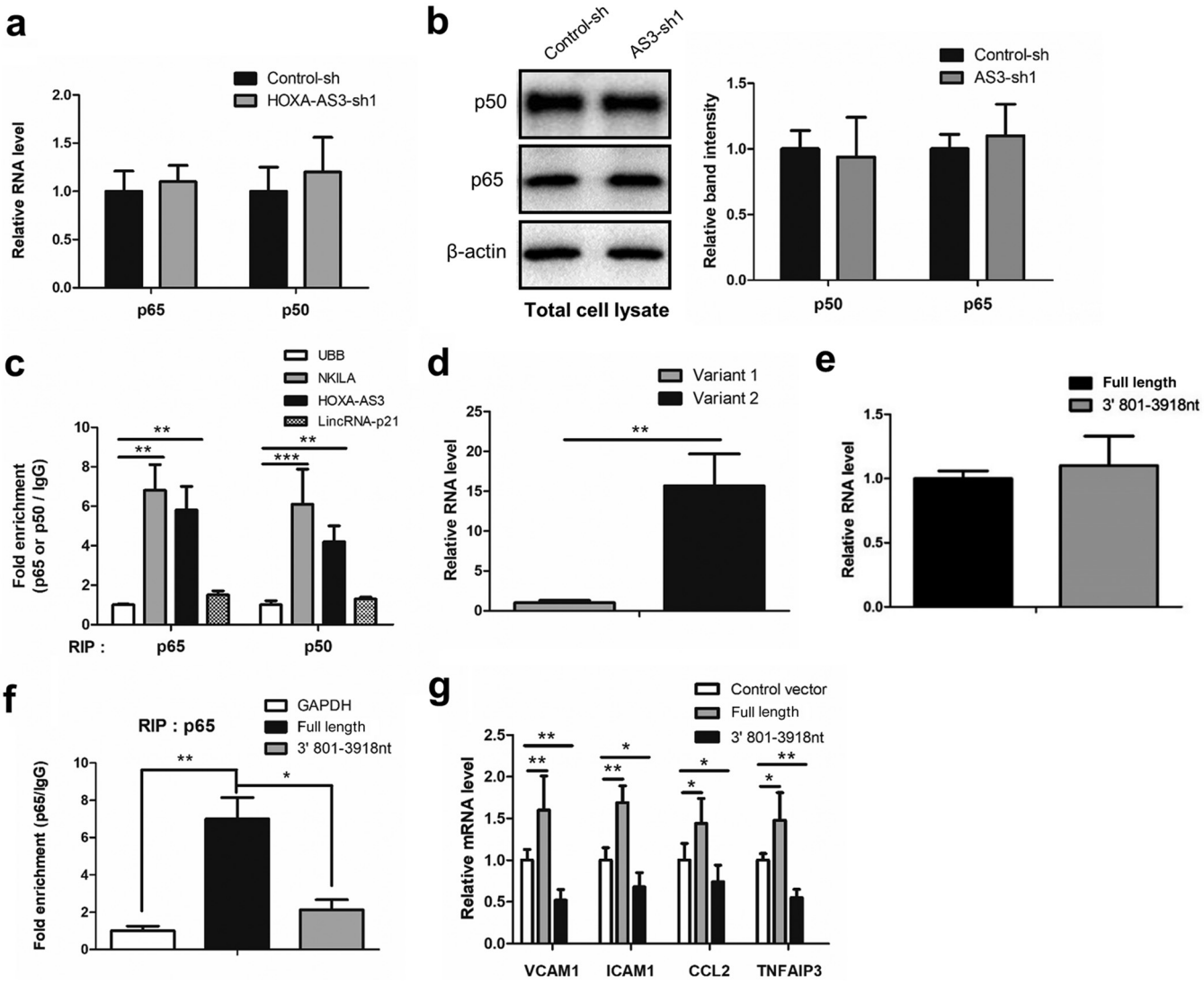

FIG 3 The 5′-terminal region of HOXA-AS3 from nt 1 to 800 interacts with NF-κB. (a) Both p65 and p50 mRNA expression levels in HUVECs with or without HOXA-AS3 knockdown were assayed by qRT-PCR. (b) Both p65 and p50 protein expression levels in HUVECs with or without HOXA-AS3 knockdown were assayed by Western blotting (left) and then quantified by using ImageJ software (right). (c) Anti-p65 and anti-p50 RNA immunoprecipitation (RIP) assays were conducted in HUVECs. The immunoprecipitated RNAs were subjected to qRT-PCR analysis to examine the association of HOXA-AS3 with NF-κB. (d) The relative expression levels of two transcript variants of HOXA-AS3 in HUVECs were measured by qRT-PCR. (e) qRT-PCR analysis showing that the exogenous full-length HOXA-AS3 and HOXA-AS3 from which nt 1 to 800 of the 5′-terminal region was deleted were expressed at similar levels in HUVECs. (f) Effect of the 5′-terminal region of HOXA-AS3 from nt 1 to 800 on its association with NF-κB, determined by anti-p65 RIP assays, followed by subsequent qRT-PCR analysis. The exogenous full-length HOXA-AS3 and HOXA-AS3 from which the 5′-terminal region from nt 1 to 800 was deleted were expressed at similar levels in HUVECs, as shown in panel e. GAPDH, glyceraldehyde-3-phosphate dehydrogenase. (g) Effect of full-length HOXA-AS3 and HOXA-AS3 from which the 5′-terminal region from nt 1 to 800 was deleted on the expression of representative NF-κB target genes (VCAM1, ICAM1, CCL2, and TNFAIP3 genes) in HUVECs, tested by qRT-PCR. All values are from biological triplicates, and the data shown are the mean ± SD. *, $P < 0.05$; **, $P < 0.01$; ***, $P < 0.001$.

showed that the expression of p65 and p50 (Fig. 3a and b), as well as other members of the NF-κB family (data not shown), was not influenced after HOXA-AS3 knockdown.

Increasing evidence has revealed that lncRNA can mediate the transcriptional activity of a number of chromatin regulatory complexes by serving as a scaffold or decoy to assemble with these regulators (36–38). Thus, we hypothesized that HOXA-AS3 can interact with NF-κB. To prove this hypothesis, RNA immunoprecipitation (RIP) assays were conducted in HUVECs. Consequently, RIP assay results showed that only p65 and p50 could specifically interact with endogenous HOXA-AS3 (Fig. 3c). Next, we sought to define the specific region of HOXA-AS3 that binds with NF-κB by the use of deletion mapping experiments. The human HOXA-AS3 consists of two transcript variants (variant 1 [GenBank accession number NR_038832.1] and variant 2 [GenBank

accession number NR_038831.1]) in the RefSeq database. We first examined the expression levels of the two variants of HOXA-AS3 in HUVECs by qRT-PCR analysis. We found that transcript variant 2 is the predominant transcript of HOXA-AS3 in HUVECs and is present at 15-fold higher levels than variant 1. However, transcript variant 1 had almost no expression (Fig. 3d). Next, we performed a sequence alignment of HOXA-AS3 from multiple species and identified a highly conserved 5′-terminal region of HOXA-AS3 (nucleotides [nt] 1 to 800) with 80% identity among human, mouse, and rat (data not shown). To demonstrate the requirement of this region for HOXA-AS3 assembly with NF-κB, we transfected the full-length HOXA-AS3 and two truncated mutants of HOXA-AS3 (one with nt 1 to 800 and one deficient in nt 1 to 800) into HEK293T cells and then performed anti-p65 RIP assays. As expected, RIP assays showed that the construct with the region of HOXA-AS3 from nt 1 to 800 could interact with p65, while the interaction with p65 was abolished in the mutant of HOXA-AS3 deficient in nt 1 to 800 (data not shown). This finding was further confirmed in HUVECs by using lentiviral vectors expressing full-length HOXA-AS3 and HOXA-AS3 deficient in nt 1 to 800 (Fig. 3e and f). To determine the functional involvement of the region of HOXA-AS3 from nt 1 to 800 in the regulation of NF-κB downstream-mediated genes, ectopic overexpression of full-length HOXA-AS3 and HOXA-AS3 lacking nt 1 to 800 was carried out in HUVECs using lentiviral infection. Consequently, qRT-PCR analysis showed that the full-length HOXA-AS3 markedly induced the expression of the NF-κB target genes. In contrast, the mutant deficient in nt 1 to 800 displayed an inhibitory effect on the expression of these NF-κB transcriptional targets (Fig. 3g). Collectively, these observations demonstrate that the 5′-terminal region of HOXA-AS3 from nt 1 to 800 is essential for its functional association with NF-κB.

HOXA-AS3 promotes the activation of NF-κB signaling. As shown in Fig. 2 and 3, HOXA-AS3 could especially interact with NF-κB and regulate its target gene expression. We next wanted to identify the precise molecular mechanism by which HOXA-AS3 regulates NF-κB activity. To address this issue, we first assayed whether HOXA-AS3 is functionally involved in the regulation of NF-κB nuclear translocation. Anti-p65 immunofluorescence staining showed that the knockdown of HOXA-AS3 remarkably blocked TNF-α-activated NF-κB nuclear translocation (Fig. 4a), suggesting the positive role of HOXA-AS3 in the activation of NF-κB signaling. Moreover, this result was further confirmed by a fractionation experiment (data not shown). Next, we examined the effect of HOXA-AS3 on the degradation of IκBα, an inhibitor protein of NF-κB, as well as the acetylation status at the K310 site of p65. As expected, the protein level of IκBα was augmented after HOXA-AS3 knockdown (Fig. 4b). Consistently, acetylation of the K310 site was significantly inhibited when HOXA-AS3 was depleted (Fig. 4b). The influence of HOXA-AS3 on NF-κB transcriptional activity was further confirmed by anti-p65 chromatin immunoprecipitation (ChIP) assays (Fig. 4c). Taken together, these findings suggest that HOXA-AS3 positively regulates the activation of NF-κB signaling.

Prior studies reported that multiple lncRNAs interact with chromatin to help guide or direct specific transcriptional regulators and then modulate gene expression (29, 46). Thus, we sought to determine whether HOXA-AS3 could act as a chromatin-associated scaffolding regulator to stabilize the association of NF-κB with κB enhancer elements. To test this notion, a fractionation experiment was first conducted to observe the cellular localization of HOXA-AS3. qRT-PCR quantification showed that the abundance of HOXA-AS3 distributed in the nucleus was comparable to that of HOXA-AS3 distributed in the cytoplasmic fraction (data not shown), indicating the possibility that HOXA-AS3 acts as a chromatin modifier. Next, we performed a chromatin isolation by RNA purification (ChIRP) assay to determine the ability of HOXA-AS3 to bind to chromatin with a set of probes targeting HOXA-AS3 in the presence or absence of TNF-α treatment. Interestingly, the ChIRP assay result indicated that HOXA-AS3 can especially bind to the promoters of these NF-κB transcriptional targets compared with a LacZ control probe set (Fig. 4d). More importantly, TNF-α treatment significantly augmented the HOXA-AS3 association with these promoters (Fig. 4d). Furthermore, an

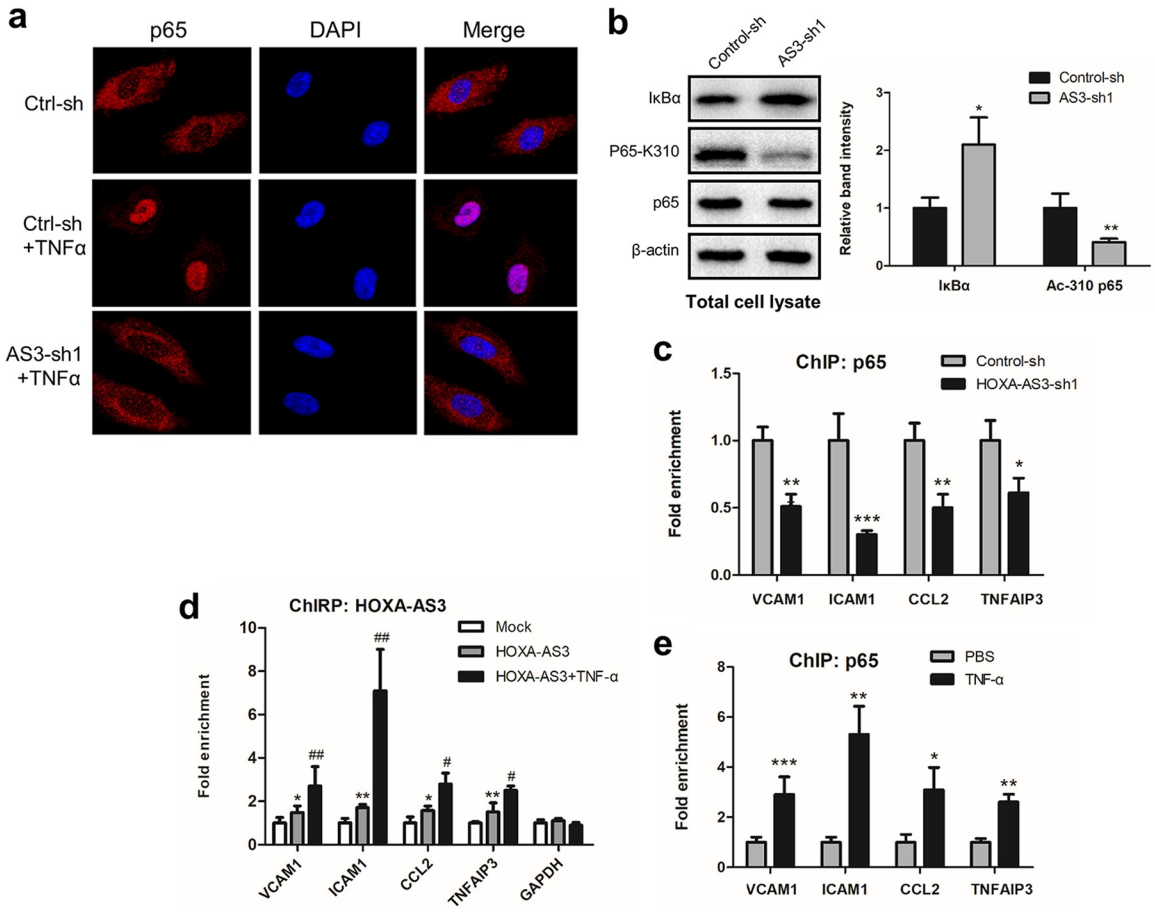

FIG 4 HOXA-AS3 is involved in NF-κB-mediated transcription elongation. (a) Effect of HOXA-AS3 on NF-κB nuclear translocation, examined by immunofluorescence staining of p65 in control and HOXA-AS3-depleted HUVECs with or without TNF-α treatment (10 ng/ml, 1 h). DAPI, 4′,6-diamidino-2-phenylindole. (b) Western blot analysis was performed in HUVECs with or without HOXA-AS3 depletion to detect the expression of IκBα and the K310 site acetylation status of p65 (left), and then the results were quantified by using ImageJ software (right). (c) ChIP assays with antibody against p65 were performed in control and HOXA-AS3-silenced HUVECs activated with TNF-α for 1 h to examine the effect of HOXA-AS3 on the distribution of p65 at the promoters of the NF-κB target genes. (d) Binding ability of HOXA-AS3 with the promoters of VCAM1, ICAM1, CCL2, and TNFAIP3 in HUVECs, assayed by ChIRP-quantitative PCR in the presence or absence of TNF-α treatment. A set of probes targeting LacZ RNA was used as a mock-transfected control. (e) An anti-p65 ChIP assay was performed in HUVECs with or without TNF-α treatment to show the TNF-α-induced NF-κB enrichment at the promoters of VCAM1, ICAM1, CCL2, and TNFAIP3. All values are from biological triplicates, and the data shown are the mean ± SD. *, $P < 0.05$ versus control shRNA-transfected, mock-transfected, or PBS-transfected cells; **, $P < 0.01$ versus control shRNA-transfected, mock-transfected, or PBS-transfected cells; ***, $P < 0.001$ versus control shRNA-transfected, mock-transfected, or PBS-transfected cells; #, $P < 0.05$ versus HOXA-AS3; ##, $P < 0.01$ versus HOXA-AS3.

anti-p65 ChIP assay was carried out to examine the colocalization of HOXA-AS3 with NF-κB at specific gene promoters. The ChIP assay data showed remarkably enriched occupancies of p65 at the promoters of the four NF-κB target genes upon TNF-α treatment (Fig. 4e), and these were identical to the distributions of HOXA-AS3. In summary, these observations suggest that HOXA-AS3, a partner of NF-κB, can function as a chromatin-associated scaffolding regulator to direct NF-κB recruitment and may stabilize NF-κB binding to κB enhancer elements.

HOXA-AS3 has a positive correlation with inflammatory atherosclerosis. The results presented above showed the crucial role of HOXA-AS3 in the regulation of endothelium inflammation. Hence, we asked whether HOXA-AS3 expression correlated with inflammatory vascular disorders. To test this hypothesis, we isolated the total RNAs of peripheral blood mononuclear cells (PBMCs) derived from patients diagnosed with carotid artery atherosclerosis and an age-matched healthy control group and then measured the expression of HOXA-AS3 using qRT-PCR assays. We found that the expression of HOXA-AS3 was dramatically elevated in patients with atherosclerotic

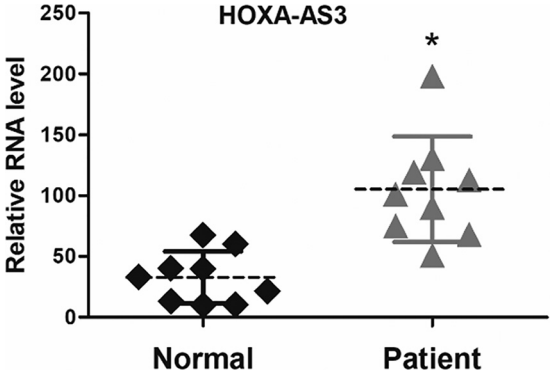

FIG 5 HOXA-AS3 positively correlated with inflammatory atherosclerotic lesions. RNA isolated from peripheral blood mononuclear cells from atherosclerotic and healthy control patients was subjected to qRT-PCR to examine the changes in the expression of HOXA-AS3. The solid and dashed horizontal lines represent the standard deviation (SD) and the mean, respectively ($n = 9$ for each experimental group). *, $P < 0.05$ versus healthy control patients (Normal); **, $P < 0.01$ versus healthy control patients.

lesions compared with that in the healthy control group (Fig. 5), suggesting a significant positive correlation of HOXA-AS3 with inflammatory atherosclerosis.

DISCUSSION

It is well reported that endothelium inflammation, critically associated with multiple vascular disorders, can be regulated by a variety of regulators, including some key transcription factors, as well as lncRNAs. In this study, we identified lncRNA HOXA-AS3 to be a critical regulator of endothelium inflammation. Attenuation of HOXA-AS3 could markedly repress monocyte adhesion to endothelial cells (ECs) and monocyte transendothelial migration *in vitro*. Moreover, HOXA-AS3 inhibition dramatically reduced the expression of adhesion molecules, such as VCAM1 and ICAM1, which could help attract monocytes and facilitate its adhesion to ECs. To determine the significant correlation between HOXA-AS3 and inflammatory vascular diseases, peripheral blood mononuclear cells derived from patients diagnosed with carotid artery atherosclerosis were isolated and then subjected to assessment of their HOXA-AS3 expression. Notably, samples from atherosclerotic patients were found to have obviously elevated HOXA-AS3 expression relative to that by samples from healthy age-matched controls. This finding proved a critical positive correlation of HOXA-AS3 with inflammatory vascular disorders, and we conclude that HOXA-AS3 may serve as an important biomarker in the clinical diagnosis of atherosclerosis and other inflammatory vascular diseases.

As one of the most important inflammatory signaling pathways, the NF-κB pathway is critically involved in multiple inflammation-associated vascular disorders, especially atherosclerosis. Aberrant activation of NF-κB can induce the expression of a number of inflammatory factors and subsequent endothelium inflammation in the early stage of atherosclerosis. Therefore, the regulation of NF-κB activity is one of the most crucial events protecting the endothelium from inflammatory lesions. Here, using an unbiased RNA sequencing approach, we discovered that HOXA-AS3 can especially modulate the expression of NF-κB transcriptional targets, including some key inflammatory factors involved in the regulation of endothelium inflammation. In the biochemical studies described here, we characterized HOXA-AS3 to be a positive regulator of NF-κB signaling. Depletion of HOXA-AS3 dramatically inhibited the transcriptional activity of NF-κB by controlling the expression of IκBα and the acetylation status of p65 at the K310 site (Fig. 6). In addition, we found that HOXA-AS3 can function as a scaffolding regulator to help recruit NF-κB to its target gene promoters by interacting with NF-κB (Fig. 6). Using a deletion mapping experiment, we prove that the 5′-terminal region of HOXA-AS3 from nt 1 to 800 is responsible for its assembly with NF-κB and the regulation of NF-κB activity, indicating that the region of HOXA-AS3 from nt 1 to 800 may be a promising therapeutic target for the treatment of multiple NF-κB-mediated inflammatory disorders.

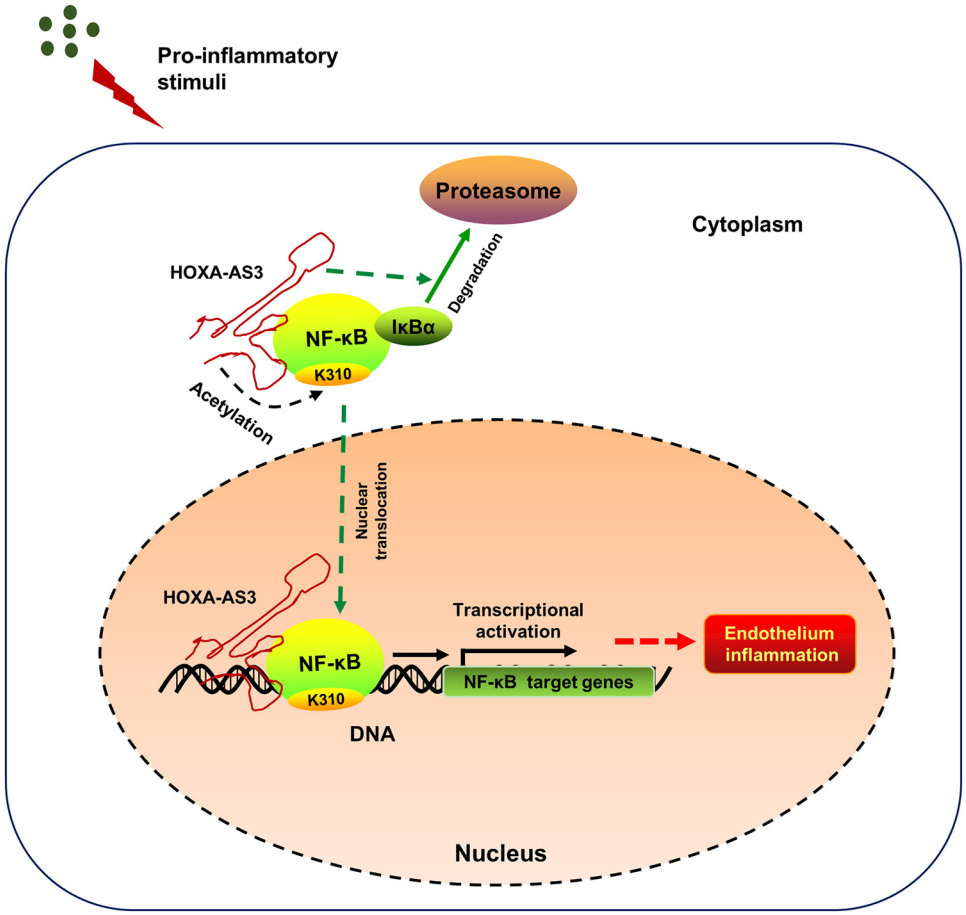

FIG 6 Schematic representation of HOXA-AS3-mediated transcriptional activation of NF-κB. When exposed to proinflammatory stimuli, intracellular HOXA-AS3 facilitates the proteasome-mediated degradation of the inhibitor protein IκBα, on the one hand. On the other hand, HOXA-AS3 promotes the acetylation of p65 at the K310 site, liberating and helping transfer NF-κB into the nucleus for transcription regulation. As a chromatin-associated scaffolding regulator, the 5′-terminal region of HOXA-AS3 from nt 1 to 800 interacts with the p65 subunit of NF-κB, facilitating the recruitment of NF-κB and stabilizing its association with specific gene promoters, therefore inducing the expression of numerous NF-κB-targeted inflammatory factors and, finally, leading to endothelium inflammation and subsequent inflammatory vascular disorders.

MATERIALS AND METHODS

Cell culture and transfection. Human umbilical vein endothelial cells (HUVECs) were cultured in complete endothelial cell medium (ECM; ScienCell Research Laboratories, Carlsbad, CA). Human THP-1 monocytes and human embryonic kidney (HEK293T) cells were cultured in RPMI medium (HyClone) and Dulbecco modified Eagle medium (Gibco) medium, respectively, supplemented with 10% (vol/vol) fetal calf serum (Gibco) and 100 units ml^{-1} streptomycin and penicillin (Millipore, Billerica, MA) at 37°C in a humidified 5% CO_2 incubator. HUVECs and THP-1 cells were purchased form ScienCell Research Laboratories (Carlsbad, CA). HEK293T cells were purchased form the American Type Culture Collection (Manassas, VA). For transfection, HEK293T cells were transiently transfected with the plasmids indicated below using a polyethyleneimine transfection protocol as previously described (39).

Antibodies and reagents. Anti-p65 antibody (catalog number sc-109) was purchased form Santa Cruz, anti-β-actin antibody (catalog number A1987) was from Sigma, and anti-VCAM1 (catalog number 60299-1-Ig) and anti-TNFAIP3 (catalog number 23456-1-AP) antibodies were from Proteintech. Anti-Brd4 and CDK9 antibodies were reported previously (40). The chemical reagent TNF-α (catalog number H8916) was obtained from Sigma, and 5-chloromethylfluorescein diacetate (CMFDA; CellTracker Green; catalog number C2925) was purchased from Invitrogen.

RNA isolation, qRT-PCR, and unbiased RNA sequencing. Total RNAs were isolated by using the TRIzol reagent. Reverse transcription (RT) was performed using a quantitative PCR (qPCR) RT kit (FSQ-201) purchased from Toyobo, and quantitative real-time PCR (qRT-PCR) was performed using an EvaGreen qPCR master mix from Applied Biological Materials Inc.; both procedures were performed according to the manufacturer's instructions. The corresponding sequences of the qRT-PCR primers are listed in Table 1.

For RNA sequencing experiments, total RNAs were extracted using the TRIzol reagent and then subjected to library construction according to standard Illumina protocols. The libraries were sequenced

TABLE 1 Primer sequences for qRT-PCR

	Sequence (5′–3′)	
Human gene	**Forward**	**Reverse**
VCAM1 gene	CATGGAATTCGAACCCAAACA	GGCTGACCAAGACGGTTGTATC
ICAM1 gene	AGCCAACCAATGTGCTATTCAAAC	CACCTGGCAGCGTAGGGTAA
CCL2 gene	CCAGCAGCAAGTGTCCCAAAG	TGCTTGTCCAGGTGGTCCATG
TNFAIP3 gene	GAGAGCACAATGGCTGAACA	TCCAGTGTGTATCGGTGCAT
KLF4 gene	CGAACCCACACAGGTGAGAA	TACGGTAGTGCCTGGTCAGTTC
HOXA-AS3		
Variant 1 gene	AAGACGGCATCAGTGTAAGC	ATTGGGAAACTCCTCAGAGCAG
Variant 2 gene	TAGTTGCGCTTTAGCTGCTC	ATGAGAGAGGTGTCTGAAGCG
GAPDH[a] gene	CATGAGAAGTATGACAACAGCCT	AGTCCTTCCACGATACCAAAGT

[a]GAPDH, glyceraldehyde-3-phosphate dehydrogenase.

with an Illumina HigSeq×Ten sequence platform and the paired-end RNA sequencing approach. For data analysis, raw reads were aligned to the reference genome, using the HTSeq-Count program, and processed by using the Cufflinks tool, which uses the normalized RNA sequencing fragment counts to measure the relative abundances of the transcripts.

RIP assay. Approximately 10^7 cells were harvested using a cell scraper and then washed with phosphate-buffered saline (PBS) three times. The cell pellets were resuspended with 1 ml buffer A (10 mM HEPES [pH 7.5], 1.5 mM $MgCl_2$, 10 mM KCl, 1.0 mM dithiothreitol [DTT], 0.5 mM phenylmethylsulfonyl fluoride [PMSF], 1× protease inhibitor cocktail) and centrifuged at 1,000 × *g* for 5 min. The swollen cells were resuspended and lysed with 0.8 ml RNA immunoprecipitation (RIP) buffer (30 mM HEPES [pH 7.5], 1.5 mM $MgCl_2$, 0.3 M NaCl, 20% glycerol, 0.5% NP-40, 1.0 mM DTT, 0.5 mM PMSF). The debris was pelleted by centrifugation at 13,000 rpm for 10 min, and the supernatants were collected and incubated with anti-p65 antibody or rabbit IgG for 4 h at 4°C with gentle rotation. Thirty microliters of protein A beads was added, and the mixture was incubated for 1 h at 4°C with gentle rotation. The immunoprecipitates were washed three times with RIP buffer and an additional two times with a high-salt buffer (50 mM Tris-HCl [pH 7.5], 300 mM NaCl, 1 mM EDTA, 1% Triton X-100, 0.1% SDS, 0.5 mM PMSF). The coimmunoprecipitated RNA was extracted and analyzed by qRT-PCR.

ChIP. Chromatin immunoprecipitation (ChIP) assays were performed as previously described (41), and the immunoprecipitated DNA was analyzed by qRT-PCR. The corresponding sequences used for the ChIP assays are presented in Table 2.

Monocyte adhesion assay. HUVECs infected with lentiviral particles expressing the short hairpin RNAs (shRNAs) indicated below were seeded in a 6-well plate. When the cells had grown to full confluence, TNF-α (10 ng/ml) was added and the mixture was incubated with the HUVEC monolayer for 3 h. In parallel, THP-1 monocytes were prelabeled with 8 μM 5-chloromethylfluorescein diacetate (CMFDA; CellTracker Green; Invitrogen) at 37°C for 30 min according to the manufacturer's instructions. Each well of HUVECs was exposed to the 0.2 ml CMFDA-labeled THP-1 cells (10^7 cells/ml) and incubated at 37°C for 2 h. After incubation, each well was washed three times with 2.0 ml ECM, adherent monocytes were imaged by fluorescence microscopy, and quantification was done by the use of ImageJ software.

ChIRP. Chromatin isolation by RNA purification (ChIRP) assays were performed in HUVECs as previously reported (42), and the immunoprecipitated DNA was analyzed by qRT-PCR.

Plasmid constructions and lentiviral infection. The short hairpin RNAs (shRNAs) targeting human HOXA-AS3 (AS3-sh) were cloned into a modified pLV-H1-Puro lentiviral vector (41), and the corresponding sequences were 5′-AAGGGCCGAACAACTCATAAA-3′ (for shRNA targeting HOXA-AS3 transcript variant 1 [AS3-sh1]) and 5′-AGCCAGGTTGCGAGTTGCAAA-3′ (for shRNA targeting HOXA-AS3 transcript variant 2 [AS3-sh2]). The full-length and truncated mutants of human HOXA-AS3 were inserted into a modified pLV-EF1α lentiviral vector as previously described (43). For lentiviral infection, experimental procedures were conducted in HUVECs or THP-1 cells as previously described (43).

Clinical inclusion criteria. All clinical PBMC samples used in this study were obtained with informed consent from the First Affiliated People's Hospital of Xinxiang Medical University. The study protocols for clinicopathological sample analysis met the standards set by the Declaration of Helsinki and were approved by the Xinxiang Medical University Review Board. The carotid artery atherosclerotic group, which was composed of patients with more than 80% carotid artery stenosis and a 1.5-mm intima-media

TABLE 2 Primer sequences for ChIP-quantitative PCR

	Sequence (5′–3′)	
Human gene	**Forward**	**Reverse**
VCAM1 gene	AAATCAATTCACATGGCATA	GACAATGCTGATTGCAGAATG
ICAM1 gene	TGTTCCCAGGTGAGTCGGGGTG	AGGTATGCAGGGTCTGGATTC
CCL2 gene	AGTTGCCTGATCTATAACATG	GCTCATTCAAATGCAGAATAG
TNFAIP3 gene	TCCCTTCTTCTTCTCCACAG	CCTGGGCATTTCGGAAGCTG

TABLE 3 Atherosclerotic patient characteristics

Patient no.	Sex	Age (yr)	Maximum IMT (mm)	hs-CRP[a] concn (mg/liter)
1	Male	68	3.5	16.8
2	Male	67	2.2	12.6
3	Male	71	3.1	13.5
4	Male	62	2.7	13.1
5	Male	58	1.8	8.6
6	Female	66	2.1	11.3
7	Female	72	1.7	7.9
8	Female	59	3	14.2
9	Female	56	1.5	7.4

[a]hs-CRP, high-sensitivity C-reactive protein.

thickness (IMT) of the carotid artery, and the healthy control group, which consisted of individuals without clinically significant carotid artery occlusion, were recruited. Peripheral blood mononuclear cells were isolated by flow cytometry, RNAs were extracted with the TRIzol reagent, and the HOXA-AS3 expression level was assayed by qRT-PCR. Detailed information about the patients is shown in Table 3.

Statistical analysis. Three different HUVEC batches were used in this study, and the HUVECs were used up to, at most, the fifth passage. Student's *t* test was used to compare two groups. For comparison of ≥3 groups, one-way analysis of variance followed by the Tukey *post hoc* test was used. The correlation of HOXA-AS3 expression and clinicopathological characteristics was analyzed by the chi-square test. A P value of <0.05 was considered statistically significant. All data are representative of those from at least three independent experiments and are presented as the mean ± standard deviation (SD).

Data availability. The RNA sequencing data have been deposited in the Sequence Read Archive (SRA) database with accession number SRP174862.

ACKNOWLEDGMENTS

This work was supported by grants from the National Natural Science Foundation of China (grants 81500354, 31502045, and 81600987) and the Shenzhen Science Foundation (grants JCYJ20160308104109234 and KQJSCX20170728150303243).

Yizhou Jiang and Xinxing Zhu conceived and designed the project. Xinxing Zhu, Duchu Chen, Yanli Liu, and Jinjin Yu performed most of the experiments. Genshen Zhong helped to analyze the clinicopathological samples. Liang Qiao, Yize Wang, and Xinqi Zhong contributed to data collections. Shuibin Lin and Demeng Chen performed statistical analysis. Xinxing Zhu wrote the draft of the manuscript. Xifeng Lu and Jieqi Wen helped revise the manuscript. All authors contributed to discussions.

We declare that there is no conflict of interest.

REFERENCES

1. Celık T, Balta S, Karaman M, Ahmet Ay S, Demırkol S, Ozturk C, Dınc M, Unal HU, Yılmaz MI, Kılıc S, Kurt G, Tas A, Iyısoy A, Quartı-Trevano F, Fıcı F, Grassı G. 2015. Endocan, a novel marker of endothelial dysfunction in patients with essential hypertension: comparative effects of amlodipine and valsartan. Blood Press 24:55–60. https://doi.org/10.3109/08037051.2014.972816.
2. Choi BJ, Matsuo Y, Aoki T, Kwon TG, Prasad A, Gulati R, Lennon RJ, Lerman LO, Lerman A. 2014. Coronary endothelial dysfunction is associated with inflammation and vasa vasorum proliferation in patients with early atherosclerosis. Arterioscler Thromb Vasc Biol 34:2473–2477. https://doi.org/10.1161/ATVBAHA.114.304445.
3. Kosmas CE, Silverio D, Tsomidou C, Salcedo MD, Montan PD, Guzman E. 2018. The impact of insulin resistance and chronic kidney disease on inflammation and cardiovascular disease. Clin Med Insights Endocrinol Diabetes 11:1179551418792257. https://doi.org/10.1177/1179551418792257.
4. Feaver RE, Gelfand BD, Wang C, Schwartz MA, Blackman BR. 2010. Atheroprone hemodynamics regulate fibronectin deposition to create positive feedback that sustains endothelial inflammation. Circ Res 106:1703–1711. https://doi.org/10.1161/CIRCRESAHA.109.216283.
5. Thomas JA, Deaton RA, Hastings NE, Shang Y, Moehle CW, Eriksson U, Topouzis S, Wamhoff BR, Blackman BR, Owens GK. 2009. PDGF-DD, a novel mediator of smooth muscle cell phenotypic modulation, is upregulated in endothelial cells exposed to atherosclerosis-prone flow patterns. Am J Physiol Heart Circ Physiol 296:H442–H452. https://doi.org/10.1152/ajpheart.00165.2008.
6. Ruland J. 2011. Return to homeostasis: downregulation of NF-kappaB responses. Nat Immunol 12:709–714. https://doi.org/10.1038/ni.2055.
7. Hayden MS, Ghosh S. 2011. NF-kappaB in immunobiology. Cell Res 21:223–244. https://doi.org/10.1038/cr.2011.13.
8. Gilmore TD, Wolenski FS. 2012. NF-kappaB: where did it come from and why? Immunol Rev 246:14–35. https://doi.org/10.1111/j.1600-065X.2012.01096.x.
9. Ghosh S, May MJ, Kopp EB. 1998. NF-kappa B and Rel proteins: evolutionarily conserved mediators of immune responses. Annu Rev Immunol 16:225–260. https://doi.org/10.1146/annurev.immunol.16.1.225.
10. Baldwin AS, Jr. 1996. The NF-kappa B and I kappa B proteins: new discoveries and insights. Annu Rev Immunol 14:649–683. https://doi.org/10.1146/annurev.immunol.14.1.649.
11. Sun X, Belkin N, Feinberg MW. 2013. Endothelial microRNAs and atherosclerosis. Curr Atheroscler Rep 15:372. https://doi.org/10.1007/s11883-013-0372-2.
12. Galkina E, Ley K. 2007. Vascular adhesion molecules in atherosclerosis. Arterioscler Thromb Vasc Biol 27:2292–2301. https://doi.org/10.1161/ATVBAHA.107.149179.
13. Byeon HE, Park BK, Yim JH, Lee HK, Moon EY, Rhee DK, Pyo S. 2012. Stereocalpin A inhibits the expression of adhesion molecules in activated vascular smooth muscle cells. Int Immunopharmacol 12:315–325. https://doi.org/10.1016/j.intimp.2011.11.020.
14. Chen F, Castranova V, Shi X. 2001. New insights into the role of nuclear factor-kappaB in cell growth regulation. Am J Pathol 159:387–397. https://doi.org/10.1016/s0002-9440(10)61708-7.

15. Bours V, Bonizzi G, Bentires-Alj M, Bureau F, Piette J, Lekeux P, Merville M. 2000. NF-kappaB activation in response to toxical and therapeutical agents: role in inflammation and cancer treatment. Toxicology 153:27–38. https://doi.org/10.1016/S0300-483X(00)00302-4.
16. Yang CR, Hsieh SL, Ho FM, Lin WW. 2005. Decoy receptor 3 increases monocyte adhesion to endothelial cells via NF-kappa B-dependent up-regulation of intercellular adhesion molecule-1, VCAM-1, and IL-8 expression. J Immunol 174:1647–1656. https://doi.org/10.4049/jimmunol.174.3.1647.
17. Mamputu JC, Renier G. 2004. Advanced glycation end-products increase monocyte adhesion to retinal endothelial cells through vascular endothelial growth factor-induced ICAM-1 expression: inhibitory effect of antioxidants. J Leukoc Biol 75:1062–1069. https://doi.org/10.1189/jlb.0603265.
18. Gerszten RE, Garcia-Zepeda EA, Lim YC, Yoshida M, Ding HA, Gimbrone MA, Jr, Luster AD, Luscinskas FW, Rosenzweig A. 1999. MCP-1 and IL-8 trigger firm adhesion of monocytes to vascular endothelium under flow conditions. Nature 398:718–723. https://doi.org/10.1038/19546.
19. Capasso R, Sambri I, Cimmino A, Salemme S, Lombardi C, Acanfora F, Satta E, Puppione DL, Perna AF, Ingrosso D. 2012. Homocysteinylated albumin promotes increased monocyte-endothelial cell adhesion and up-regulation of MCP1, Hsp60 and ADAM17. PLoS One 7:e31388. https://doi.org/10.1371/journal.pone.0031388.
20. Huang B, Yang XD, Zhou MM, Ozato K, Chen LF. 2009. Brd4 coactivates transcriptional activation of NF-kappaB via specific binding to acetylated RelA. Mol Cell Biol 29:1375–1387. https://doi.org/10.1128/MCB.01365-08.
21. Liu B, Sun L, Liu Q, Gong C, Yao Y, Lv X, Lin L, Yao H, Su F, Li D, Zeng M, Song E. 2015. A cytoplasmic NF-kappaB interacting long noncoding RNA blocks IkappaB phosphorylation and suppresses breast cancer metastasis. Cancer Cell 27:370–381. https://doi.org/10.1016/j.ccell.2015.02.004.
22. Lu Z, Li Y, Wang J, Che Y, Sun S, Huang J, Chen Z, He J. 2017. Long non-coding RNA NKILA inhibits migration and invasion of non-small cell lung cancer via NF-kappaB/Snail pathway. J Exp Clin Cancer Res 36:54. https://doi.org/10.1186/s13046-017-0518-0.
23. Wu G, Cai J, Han Y, Chen J, Huang ZP, Chen C, Cai Y, Huang H, Yang Y, Liu Y, Xu Z, He D, Zhang X, Hu X, Pinello L, Zhong D, He F, Yuan GC, Wang DZ, Zeng C. 2014. LincRNA-p21 regulates neointima formation, vascular smooth muscle cell proliferation, apoptosis, and atherosclerosis by enhancing p53 activity. Circulation 130:1452–1465. https://doi.org/10.1161/CIRCULATIONAHA.114.011675.
24. Guttman M, Amit I, Garber M, French C, Lin MF, Feldser D, Huarte M, Zuk O, Carey BW, Cassady JP, Cabili MN, Jaenisch R, Mikkelsen TS, Jacks T, Hacohen N, Bernstein BE, Kellis M, Regev A, Rinn JL, Lander ES. 2009. Chromatin signature reveals over a thousand highly conserved large non-coding RNAs in mammals. Nature 458:223–227. https://doi.org/10.1038/nature07672.
25. Mattick JS. 2009. The genetic signatures of noncoding RNAs. PLoS Genet 5:e1000459. https://doi.org/10.1371/journal.pgen.1000459.
26. Reddy MA, Chen Z, Park JT, Wang M, Lanting L, Zhang Q, Bhatt K, Leung A, Wu X, Putta S, Sætrom P, Devaraj S, Natarajan R. 2014. Regulation of inflammatory phenotype in macrophages by a diabetes-induced long noncoding RNA. Diabetes 63:4249–4261. https://doi.org/10.2337/db14-0298.
27. Mercer TR, Dinger ME, Mattick JS. 2009. Long non-coding RNAs: insights into functions. Nat Rev Genet 10:155–159. https://doi.org/10.1038/nrg2521.
28. Dinger ME, Pang KC, Mercer TR, Mattick JS. 2008. Differentiating protein-coding and noncoding RNA: challenges and ambiguities. PLoS Comput Biol 4:e1000176. https://doi.org/10.1371/journal.pcbi.1000176.
29. Uchida S, Dimmeler S. 2015. Long noncoding RNAs in cardiovascular diseases. Circ Res 116:737–750. https://doi.org/10.1161/CIRCRESAHA.116.302521.
30. Li H, Zhu H, Ge J. 2016. Long noncoding RNA: recent updates in atherosclerosis. Int J Biol Sci 12:898–910. https://doi.org/10.7150/ijbs.14430.
31. Cheng HS, Njock MS, Khyzha N, Dang LT, Fish JE. 2014. Noncoding RNAs regulate NF-kappaB signaling to modulate blood vessel inflammation. Front Genet 5:422. https://doi.org/10.3389/fgene.2014.00422.
32. Kapranov P, Cheng J, Dike S, Nix DA, Duttagupta R, Willingham AT, Stadler PF, Hertel J, Hackermuller J, Hofacker IL, Bell I, Cheung E, Drenkow J, Dumais E, Patel S, Helt G, Ganesh M, Ghosh S, Piccolboni A, Sementchenko V, Tammana H, Gingeras TR. 2007. RNA maps reveal new RNA classes and a possible function for pervasive transcription. Science 316:1484–1488. https://doi.org/10.1126/science.1138341.
33. Fatica A, Bozzoni I. 2014. Long non-coding RNAs: new players in cell differentiation and development. Nat Rev Genet 15:7–21. https://doi.org/10.1038/nrg3606.
34. Motterle A, Pu X, Wood H, Xiao Q, Gor S, Ng FL, Chan K, Cross F, Shohreh B, Poston RN, Tucker AT, Caulfield MJ, Ye S. 2012. Functional analyses of coronary artery disease associated variation on chromosome 9p21 in vascular smooth muscle cells. Hum Mol Genet 21:4021–4029. https://doi.org/10.1093/hmg/dds224.
35. Congrains A, Kamide K, Oguro R, Yasuda O, Miyata K, Yamamoto E, Kawai T, Kusunoki H, Yamamoto H, Takeya Y, Yamamoto K, Onishi M, Sugimoto K, Katsuya T, Awata N, Ikebe K, Gondo Y, Oike Y, Ohishi M, Rakugi H. 2012. Genetic variants at the 9p21 locus contribute to atherosclerosis through modulation of ANRIL and CDKN2A/B. Atherosclerosis 220:449–455. https://doi.org/10.1016/j.atherosclerosis.2011.11.017.
36. Zhao J, Sun BK, Erwin JA, Song JJ, Lee JT. 2008. Polycomb proteins targeted by a short repeat RNA to the mouse X chromosome. Science 322:750–756. https://doi.org/10.1126/science.1163045.
37. Tsai MC, Manor O, Wan Y, Mosammaparast N, Wang JK, Lan F, Shi Y, Segal E, Chang HY. 2010. Long noncoding RNA as modular scaffold of histone modification complexes. Science 329:689–693. https://doi.org/10.1126/science.1192002.
38. Huarte M, Guttman M, Feldser D, Garber M, Koziol MJ, Kenzelmann-Broz D, Khalil AM, Zuk O, Amit I, Rabani M, Attardi LD, Regev A, Lander ES, Jacks T, Rinn JL. 2010. A large intergenic noncoding RNA induced by p53 mediates global gene repression in the p53 response. Cell 142:409–419. https://doi.org/10.1016/j.cell.2010.06.040.
39. Chen R, Liu M, Li H, Xue Y, Ramey WN, He N, Ai N, Luo H, Zhu Y, Zhou N, Zhou Q. 2008. PP2B and PP1alpha cooperatively disrupt 7SK snRNP to release P-TEFb for transcription in response to Ca^{2+} signaling. Genes Dev 22:1356–1368. https://doi.org/10.1101/gad.1636008.
40. Lu X, Zhu X, Li Y, Liu M, Yu B, Wang Y, Rao M, Yang H, Zhou K, Wang Y, Chen Y, Chen M, Zhuang S, Chen LF, Liu R, Chen R. 2016. Multiple P-TEFbs cooperatively regulate the release of promoter-proximally paused RNA polymerase II. Nucleic Acids Res 44:6853–6867. https://doi.org/10.1093/nar/gkw571.
41. Zhu X, Du J, Yu J, Guo R, Feng Y, Qiao L, Xu Z, Yang F, Zhong G, Liu F, Cheng F, Chu M, Lin J. 2019. LncRNA NKILA regulates endothelium inflammation by controlling a NF-kappaB/KLF4 positive feedback loop. J Mol Cell Cardiol 126:60–69. https://doi.org/10.1016/j.yjmcc.2018.11.001.
42. Chu C, Quinn J, Chang HY. 2012. Chromatin isolation by RNA purification (ChIRP). J Vis Exp 2012:3912. https://doi.org/10.3791/3912.
43. Ai N, Hu X, Ding F, Yu B, Wang H, Lu X, Zhang K, Li Y, Han A, Lin W, Liu R, Chen R. 2011. Signal-induced Brd4 release from chromatin is essential for its role transition from chromatin targeting to transcriptional regulation. Nucleic Acids Res 39:9592–9604. https://doi.org/10.1093/nar/gkr698.
44. Tong Y, Wang M, Dai Y, Bao D, Zhang J, Pan H. 17 May 2019. LncRNA HOXA-AS3 sponges miR-29c to facilitate cell proliferation, metastasis, and EMT process and activate the MEK/ERK signaling pathway in hepatocellular carcinoma. Hum Gene Ther Clin Dev https://doi.org/10.1089/humc.2018.266.
45. Wu F, Zhang C, Cai J, Yang F, Liang T, Yan X, Wang H, Wang W, Chen J, Jiang T. 2017. Upregulation of long noncoding RNA HOXA-AS3 promotes tumor progression and predicts poor prognosis in glioma. Oncotarget 8:53110–53123. https://doi.org/10.18632/oncotarget.18162.
46. Guttman M, Rinn JL. 2012. Modular regulatory principles of large non-coding RNAs. Nature 482:339–346. https://doi.org/10.1038/nature10887.